Supplementary Information for

Formation of the Ni(II)-Phenoxyl Radical Complexes by O_2: A Mechanistic Insight into the Reaction of Ni(II)-Phenol Complexes with O_2

Takashi Suzuki, Akari Sato, Hiromi Oshita, Tatsuo Yajima, Fumito Tani, Hitoshi Abe, Kaoru Mieda-Higa, Sachiko Yanagisawa and Yuichi Shimazaki*

Table of contents:

and deuterium–labelled complex **3** (red square) with O_2. The black line and the red line are fitting results of complex **3** and the deuterium–labelled complex **3**, respectively.

Table S2. Crystallographic Data for $[Ni(HtbuL)(CH_3OH)_2]ClO_4 \bullet 2CH_3OH$ (**1**), $[Ni(HMeOL)(CH_3OH)_2]ClO_4$ (**2**), $[Ni_2(tbuL)_2]$ (**4**) and $[Ni(Me_2NL)(CH_3OH)_2]ClO_4$ (**5**).

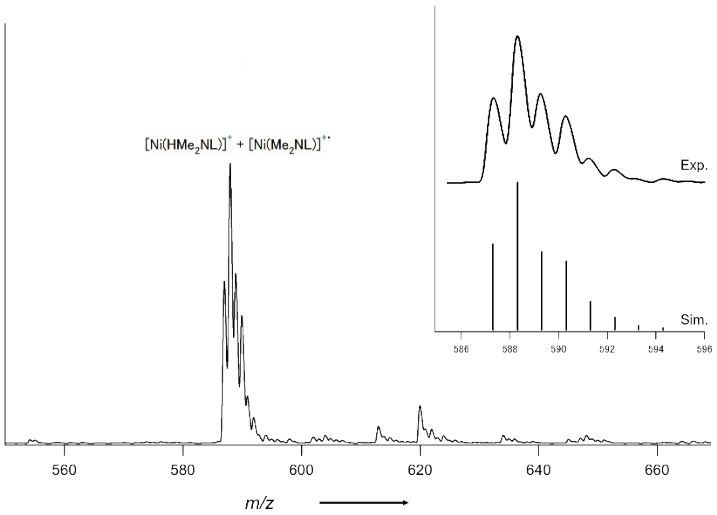

Figure S1. ESI-MS spectrum of reaction mixture of $Ni(ClO_4)_2 \cdot 6H_2O$ in CH_3OH with H_2Me_2NL in CH_2Cl_2 and 1 equivalent of triethylamine under the aerobic conditions. Inset; expand view of the spectrum in the region of $[Ni(HMe_2NL)]^+$ and the simulation. The peak was estimated to be sum of Ni^{II}-(phenol)(phenolate) complex $[Ni(HMe_2NL)]^+$ (57.1 %) and its oxidized complex $[Ni(Me_2NL)]^+$ (42.9 %), due to the oxidation by O_2 during the measurement.

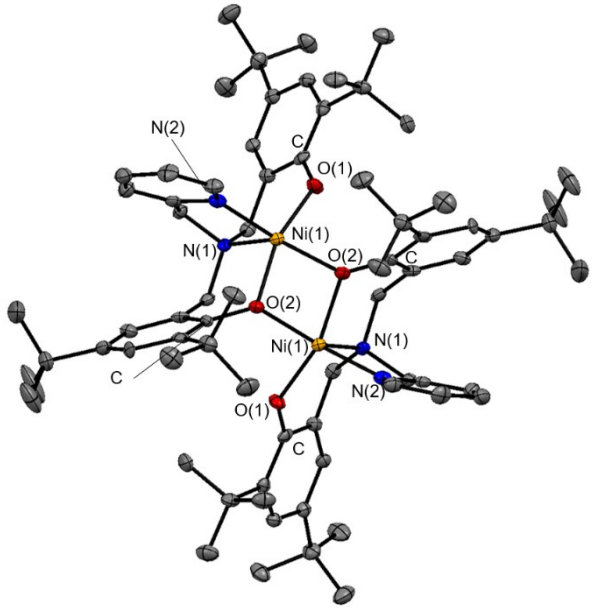

Figure S2. X-ray structure of $[Ni_2(tbuL)_2]$ (**4**).

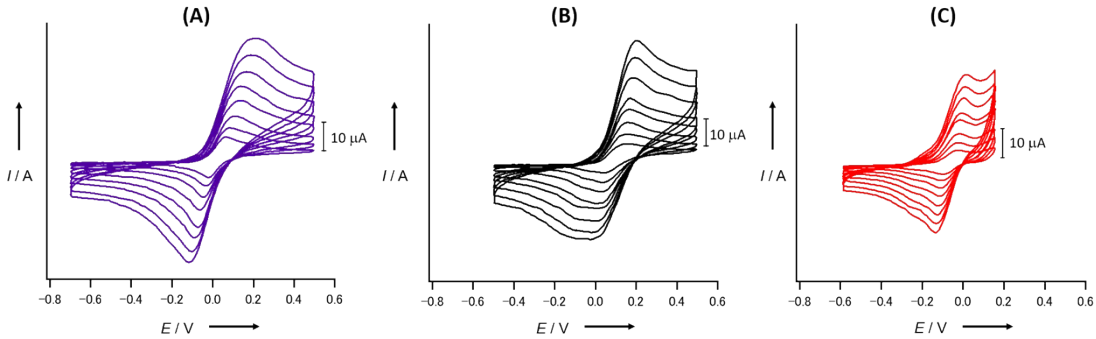

Figure S3. Cyclic voltammograms of dimer complex **4** (0.5 mM) in CH_2Cl_2 (A), complex **1** in CH_2Cl_2/CH_3OH (B) and **2** in CH_2Cl_2/CH_3OH (C) containing $[NBu_4][PF_6]$ (0.1 M) as supporting electrolyte, at scan rates of 20-1000 mV/s.

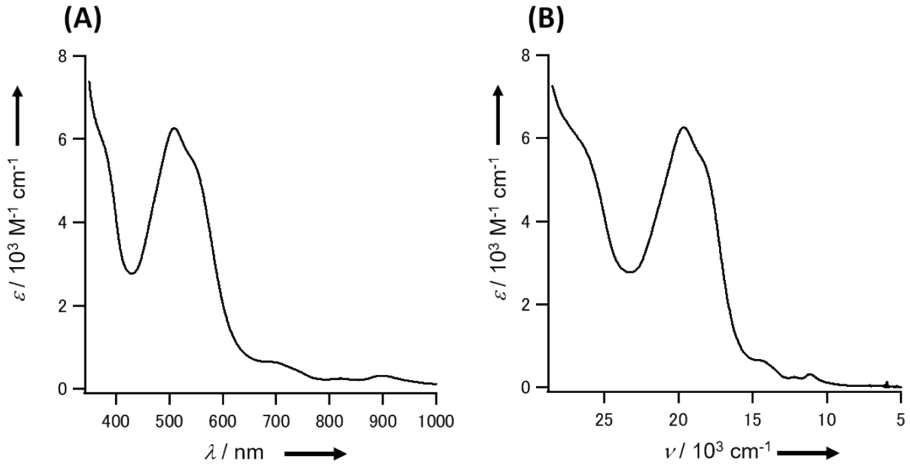

Figure S4. UV-vis-NIR spectrum of $[Ni(Me_2NL)(CH_3OH)_2]ClO_4$ (**5**) with the horizontal axis of wavelength (nm) (A) and wavenumber (cm^{-1}) (B).

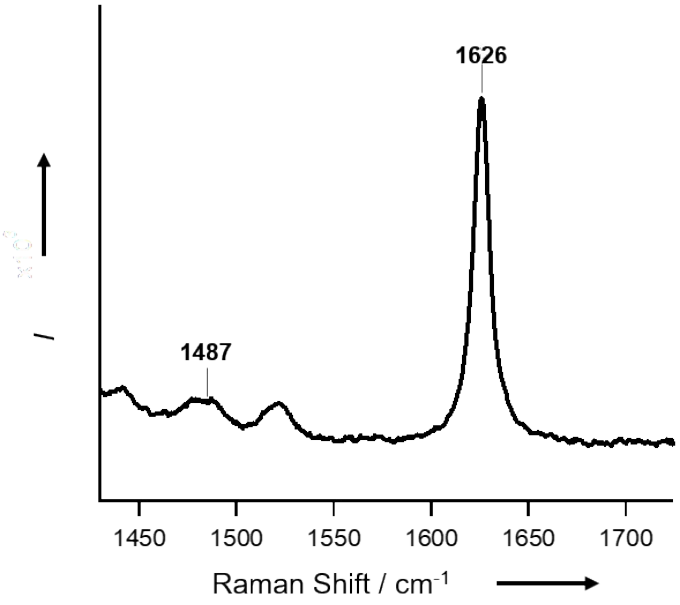

Figure S5. Resonance Raman spectrum of complex **5** in CH_2Cl_2 at λ_{ex} = 532 nm excitation.

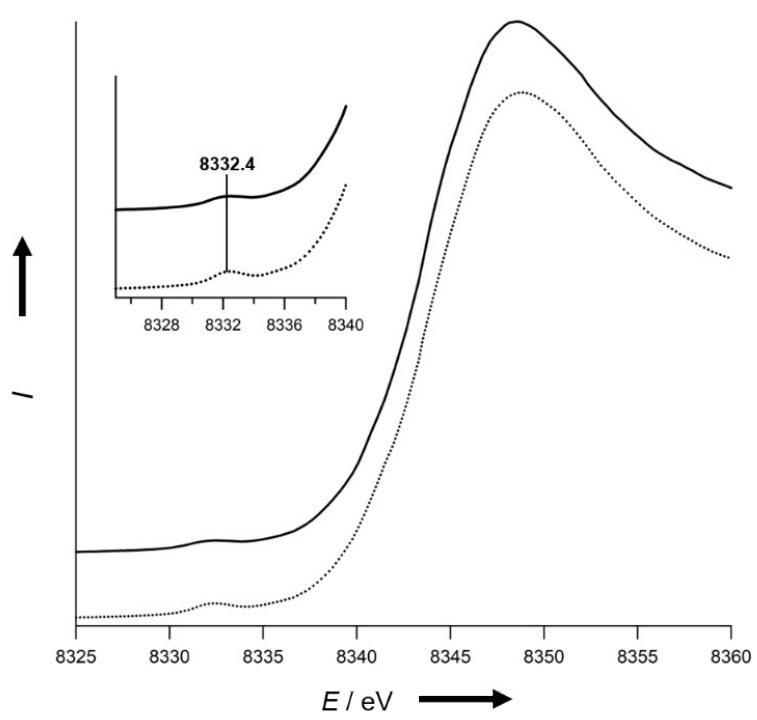

Figure S6. Ni K-edge XANES of Ni complexes **1** (dotted line) and **5** (solid line).

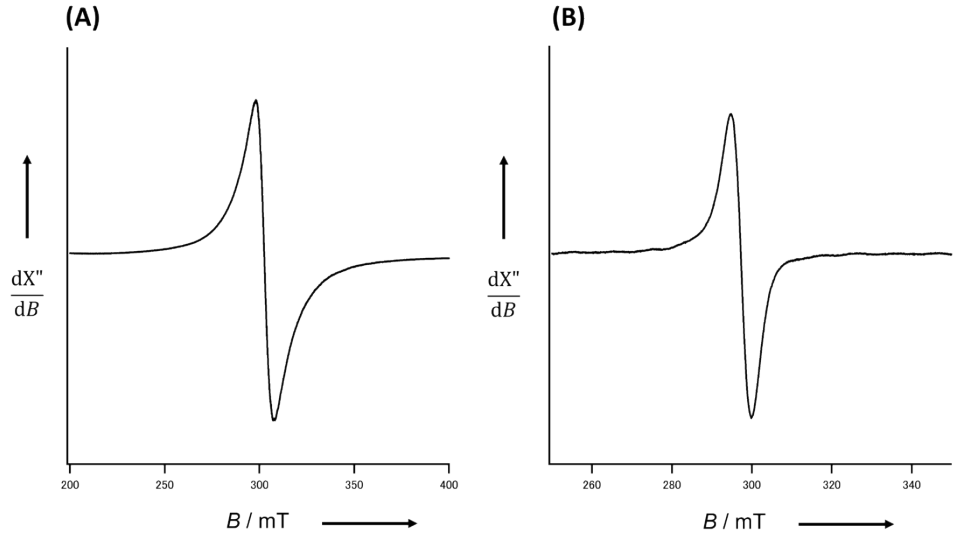

Figure S7. EPR spectra of **1** exposed to O_2 for 1 days (A) and **5** (B) in CH_2Cl_2 at 4 K.

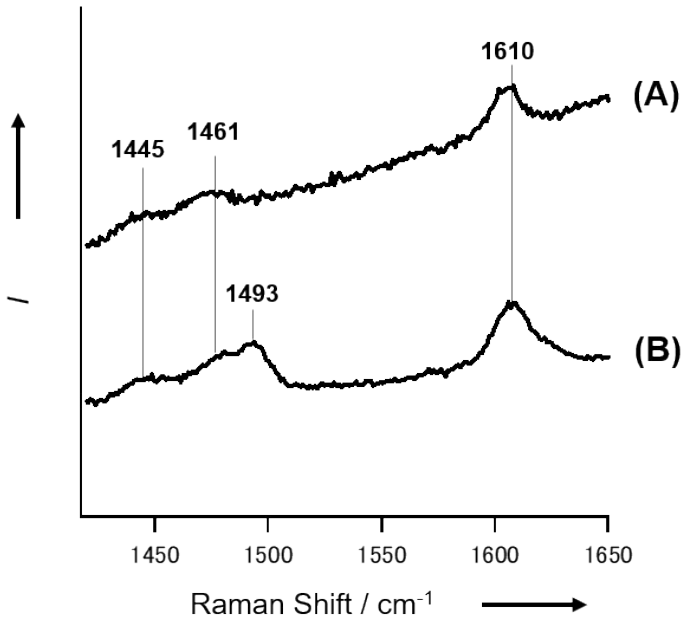

Figure S8. Resonance Raman spectra of **1** (A) and its oxidation products obtained by O_2 for 24 h (B) at λ_{ex} = 405 nm excitation.

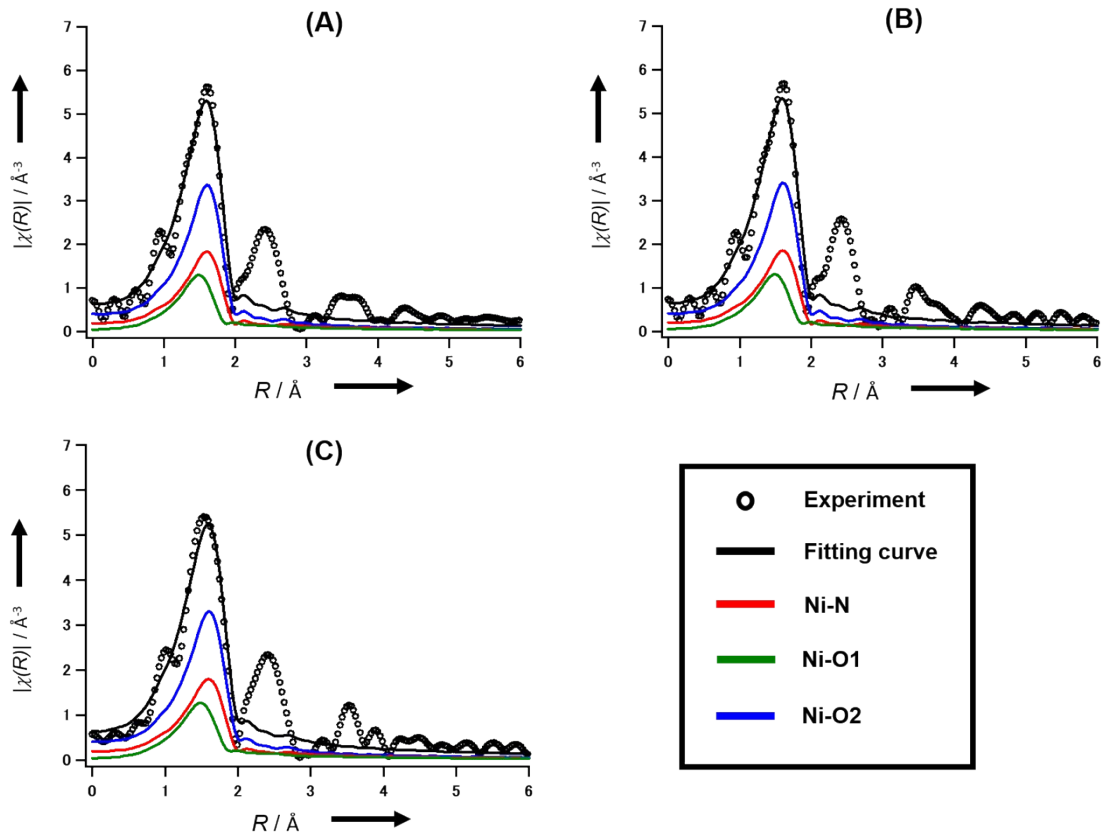

Figure S9. EXAFS curve fitting results for complex **1** (A) and its oxidized species exposed to O_2 for 6 h (B) and 24 h (C) in *R*-space. The experimental (black circle) and the fitting curve (black line) are shown in the figure. Red, green, and blue line denote the scattering paths from two Ni-N bond, one Ni-phenolate oxygen bond (Ni-O1) and three Ni-O (Ni-phenol (or Ni-phenoxyl radical) and two Ni-methanol oxygen) bond (Ni-O2), respectively. Fittings were performed for the coordination shells in the *R*-range of 1.1-2.0 Å.

Table S1. Structural parameters obtained from the EXAFS curve fittings.

Sample	Bond	Distance(Å)	CN [a]	CN (total)	DW [b] factor	*R*-factor
complex 1 (0h)	Ni-N	2.06	1.96	5.89	0.010	0.005
	Ni-O1	1.93	0.98		0.010	
	Ni-O2	2.06	2.94		0.010	
6h	Ni-N	2.06	1.97	5.92	0.010	0.006
	Ni-O1	1.93	0.99		0.010	
	Ni-O2	2.06	2.96		0.010	
24 h	Ni-N	2.06	2.09	6.26	0.011	0.005
	Ni-O1	1.93	1.04		0.011	
	Ni-O2	2.06	3.13		0.011	

[a] Coordination Number

[b] Debye-Waller

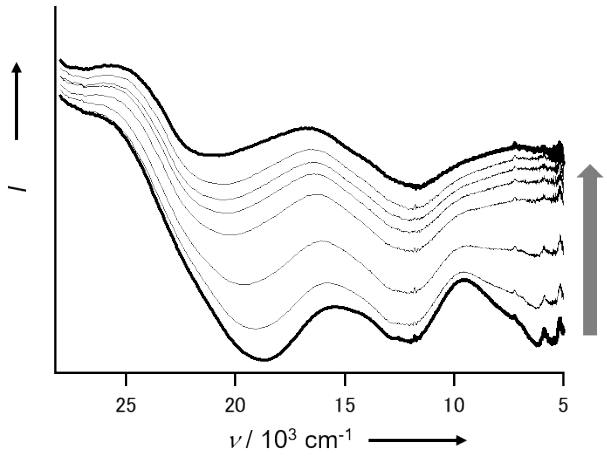

Figure S10. Reflectance spectral change for the oxidation of the deuterated complex **1** in the solid state. From the bottom line to top line, the spectra indicate 0 h, 0.5 h, 1 h, 2 h, 3 h, 4h, 6h, 24h-oxidation by O_2, respectively.

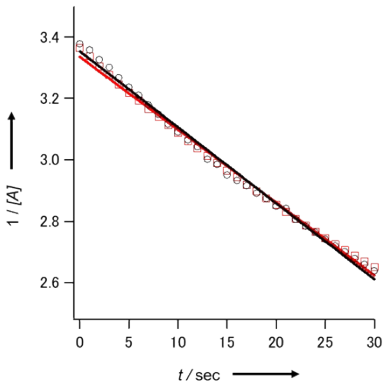

Figure S11. Plot of 1/[A] at 510 nm vs time in the initial step of complex **3** (black circle) and deuterium–labelled complex **3** (red square) with O_2 at 243 K. The black line and the red line are fitting results of complex **3** and the deuterium–labelled complex **3**, respectively.

Table S2. Crystallographic Data for $[Ni(HtbuL)(CH_3OH)_2]ClO_4 \bullet 2CH_3OH$ (**1**), $[Ni(HMeOL)(CH_3OH)_2]ClO_4$ (**2**), $[Ni_2(tbuL)_2]$ (**4**) and $[Ni(Me_2NL)(CH_3OH)_2]ClO_4$ (**5**).

	1	**2**	**4**
Formula	$C_{40}H_{58}ClN_2NiO_{10}$	$C_{35}H_{53}ClN_2NiO_9$	$C_{36}H_{50}N_2NiO_2$
Formula weight	821.06	739.96	601.50
Color	Green	Green	Yellow
Crystal size /mm	0.15 x 0.12 x 0.05	0.06 x 0.06 x 0.01	0.09 x 0.09 x 0.02
Crystal system	Triclinic	Triclinic	Monoclinic
Space group	*P* -1	*P* -1	*C*2/*c*
a (Å)	11.4551(7)	11.1065(9)	29.0820(17)
b (Å)	14.5863(9)	14.0921(11)	9.6176(5)
c (Å)	15.9271(11)	14.4840(13)	23.3195(12)
α (º)	63.7131(18)	106.612(8)	-
β (º)	71.4309(18)	110.723(8)	96.960(7)
γ (º)	68.271615)	106.927(8)	-
V (Å^3)	2178.0(2)	1826.8(4)	6474.4(6)
Z	2	2	8
μ (cm^{-1})	5.61	6.58	6.33
F(000)	874.00	788.00	2592.00
D_{calc} (g/cm^3)	1.252	1.345	1.234
$2\theta_{max}$ (°)	55.0	55.0	55.0
No. reflections obsd.	9718	8295	7425
No. reflections used.	7106	8295	7425
No. variables	532	445	370
R_1[a] ($I>2\sigma(I)$)	0.0623	0.0869	0.0757
R_w[b]	0.1806	0.2390	0.2404

Table S2. (continued)

	5
Formula	$C_{36}H_{55}ClN_3NiO_8$
Formula weight	752.00
Color	Brown
Crystal size /mm	0.10 x 0.10 x 0.10
Crystal system	Triclinic
Space group	*P* -1
a (Å)	11.2054(14)
b (Å)	14.0233(16)
c (Å)	14.5332(15)
α (º)	105.820(7)
b (Å)	110.390(8)
γ (º)	107.239(7)
V (Å^3)	1885.5(4)
Z	2
μ (cm^{-1})	6.48
F(000)	802.00
D_{calc} (g/cm^3)	1.346
$2\theta_{max}$ (°)	55.0
No. reflections obsd.	8428
No. reflections used.	8428
No. variables	450
R_1[a] ($I>2\sigma(I)$)	0.0550
R_w[b]	0.1616

[a] $R_1 = \Sigma||F_o|-|F_c|| / \Sigma|F_o|$ for $I > 2\sigma(I)$ data. [b] $R_w = \{\Sigma\omega(|F_o|-|F_c|)^2 / \Sigma\omega F_o^2\}^{1/2}$; $\omega = 1/\sigma^2(F_o) = \{\sigma^2_c(F_o) + p^2/4 \cdot F_o^2\}^{-1}$